Dynamic Disorder and Conformer Exchange in the Crystalline Monomer of Polycarbonate

J. E. Wolak,[†] J. Knutson,[†] J. D. Martin,[†] P. Boyle,[†] Andrew L. Sargent,[‡] and Jeffery L. White*,[†]

Department of Chemistry, North Carolina State University, Raleigh, North Carolina 27695-8204, and Department of Chemistry, East Carolina University, Greenville, North Carolina 27858

Received: August 25, 2003; In Final Form: September 19, 2003

Direct measurement of chemical exchange events in the crystalline polycarbonate monomer 4,4′- isopropylidenediphenol (bisphenol A, BPA) via 2D ^{13}C solid-state NMR reveals slow, large-amplitude aromatic ring reorientations. X-ray diffraction, however, indicates a static crystalline structure. Experiments with multiple exchange times show that ring flips occur in all of the three unique conformers found in the crystalline unit cell of this compound, but in specific cases, two of the three unique molecules actually switch conformations. Kinetic analysis of the exchange data indicates that the average rate constant $k_{ex} = 0.01\ s^{-1}$ for ring flips and conformer interchange at room temperature. Differential scanning calorimetry and variable-temperature powder diffraction studies indicate a systematic volume expansion that accompanies this motion but no first-order phase transition. All room-temperature exchange events may be quenched at 213 K, at least on the time scale (up to several seconds) probed in this work. Simulation of the potential-energy surface of BPA molecules reveals that the lowest-energy pathway for ring flips (maximum energy of 1.9 kcal/mol) involves +110° flips of one ring coincident with +70° flips of the second. The mechanism of the ring dynamics in the crystalline monomer is unique relative to those previously reported for the polycarbonate in that the collective motion of both rings in a monomer unit is 180°, whereas single-ring flips of 180° occur in the polymer.

Introduction

Bisphenol A (4,4′-isopropylidenediphenol or BPA) is the crystalline organic monomer of polycarbonate and, in addition, finds application in a variety of epoxy resins. The relationship between dynamics, diffusion, and elution of residual BPA monomer from polycarbonate and its overall chemical toxicity is currently receiving widespread attention in the literature due to its potential health hazards.[1] In its pure crystalline form, BPA contains three crystallographically distinct molecules in its unit cell, differing primarily in the relative orientation of the two aromatic rings in each molecule.[2−4] Intermolecular hydrogen bonding defines the overall packing of molecules in the crystal, with the characteristic self-association of phenolic compounds leading to the differential molecular configurations. X-ray crystallography provides well-defined atomic coordinates at room temperature (corresponding to the space group $P2_1/n$), as would be expected for a crystalline solid with a melting point in excess of 150 °C.[2,3] A highly crystalline solid, we (and others) initially considered solid BPA to be a control compound for rigid lattice exchange experiments. However, upon detailed examination, we have observed large-amplitude local motions associated with aromatic ring reorientation and conformer interchange at temperatures even below ambient.

Aromatic ring dynamics in the solid state have been the subject of recent investigations in the area of glassy polymers as the molecular-level, large-amplitude motions provide a possible pathway for mechanical energy dissipation. Most notably, Schaefer has demonstrated that π flips of the aromatic rings take place in glassy polycarbonates.[5−7] Using dipolar-echo solid-state NMR methods, Schaefer and co-workers identified a broad distribution of π-flip rates ranging from kHz to MHz and showed that these molecular motions are relevant to bulk mechanical relaxation in the solid state.[5] Since that time, others have corroborated the presence of aromatic ring π flips in several different types of glassy polycarbonates, some small molecule analogues, and other amorphous macromolecules such as polystyrene.[8−13] In this report, we (1) prove that specific subsets of these motions occur in the crystalline monomer, (2) identify the relevant motional amplitudes and time scales, and (3) discern the individual conformers in the unit cell which participate in exchange via these ring motions.

Experimental Section

Polycrystalline BPA was obtained from Aldrich and used without further modification for the NMR experiments. The melting point of the pure solid is 156 °C, as confirmed using a TA Instruments D-100 DSC. Pure-phase 2D $^{13}C-^{13}C$ exchange experiments were acquired using the simple 3-pulse sequence, modified for cross-polarization excitation, and, with mixing times, synchronized to the rotor period.[14−16] Typically, 128 t_1 increments were acquired using 48 scans per increment, with subsequent zero filling to generate a 1 K × 1 K data matrix prior to Fourier transformation. NMR measurements were acquired on a Bruker DSX instrument, operating at 7.05 T field strength, which corresponds to a ^{13}C resonance frequency of 75 MHz. Unless otherwise stated, magic-angle spinning (MAS) speeds were 4−5 kHz and radio-frequency field strengths were 72 kHz. Control experiments using 100-kHz continuous wave vs two-pulse phase modulation decoupling did not produce any improvements in resolution. Similar experiments at 7−8 kHz MAS on an 11.7-T system also failed to yield any improvements

* To whom all correspondence should be addressed. E-mail: jeff_l_white@ncsu.edu.
[†] North Carolina State University.
[‡] East Carolina University.

10.1021/jp036527q CCC: $25.00
Published on Web 11/06/2003

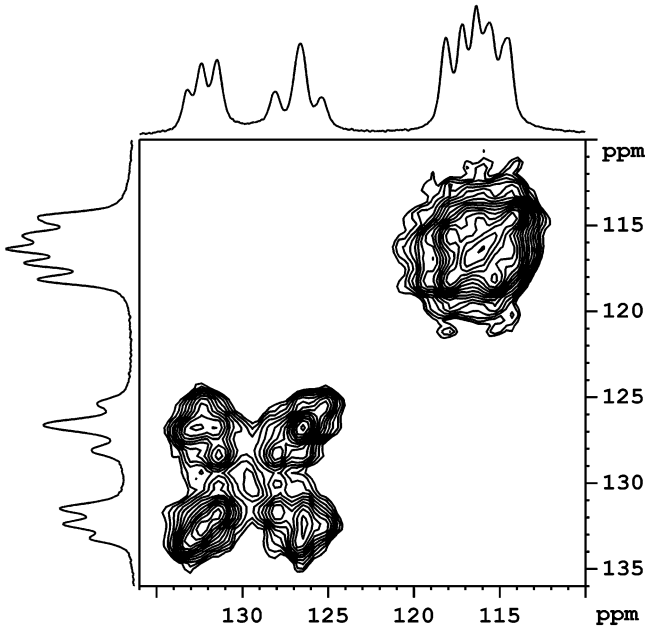

Figure 1. 2D $^{13}C-^{13}C$ exchange plot of the BPA aromatic region at 23 °C using a 1 s exchange time.

in spectral resolution. ^{1}H-mediated ^{13}C spin diffusion was ruled out as a possible polarization transfer mechanism via comparison of 2D exchange experiments with and without ^{1}H decoupling during acquisition, in which identical cross-peak volumes were obtained.[15] Cross-peak volumes were integrated for kinetic analysis of the exchange process.

Solid-state $^{1}H-^{13}C$ heteronuclear correlation experiments were acquired using Lee−Goldburg irradiation during the evolution period.[18] While the data are not presented here for brevity, several distinct and well-resolved ^{1}H chemical shifts were detected for the protonated aromatic carbons, with a total chemical shift range exceeding 1 ppm. This result is consistent with the expected intramolecular neighboring group shielding contributions to the total shift and is in agreement with the ^{13}C solid-state data (vide infra).

A solution of BPA and ethanol was prepared and allowed to slowly evaporate for two weeks. Crystals suitable for single-crystal X-ray diffraction were obtained. Single-crystal X-ray structures were obtained at −60 °C, and the results compared to published room-temperature data.[4] The sample was mounted on the end of a glass fiber using a small amount of silicon grease and transferred to the diffractometer. The sample was maintained at a temperature of −60 °C using a nitrogen cold stream. All X-ray measurements were made on an Enraf-Nonius CAD4-MACH diffractometer.

Variable-temperature powder X-ray diffraction data were collected using an INEL diffractometer. Samples were placed in 0.5-mm fused-silica capillaries and mounted on a rotating goniometer head. Samples were heated with a home-built forced-air furnace with temperature controlled to ±0.5° using an Omega controller. The powder diffraction data were calibrated to an external silicon standard, and lattice constants were determined by a least squares refinement of >20 lines.

Full-gradient geometry optimizations were performed in density functional theory (DFT) with the B3LYP wave function, as implemented in the Gaussian 98 program suite.[19] The 6-31G* basis set[20] was used throughout as a compromise between accuracy and applicability to molecules of this size. Approximate transition state geometries were evaluated with the QST2 algorithm[21] but were subsequently verified as first-order saddle points with frequency calculations at the B3LYP/6-31G* level of theory. All equilibrium structures were likewise characterized and verified to possess no imaginary frequencies.

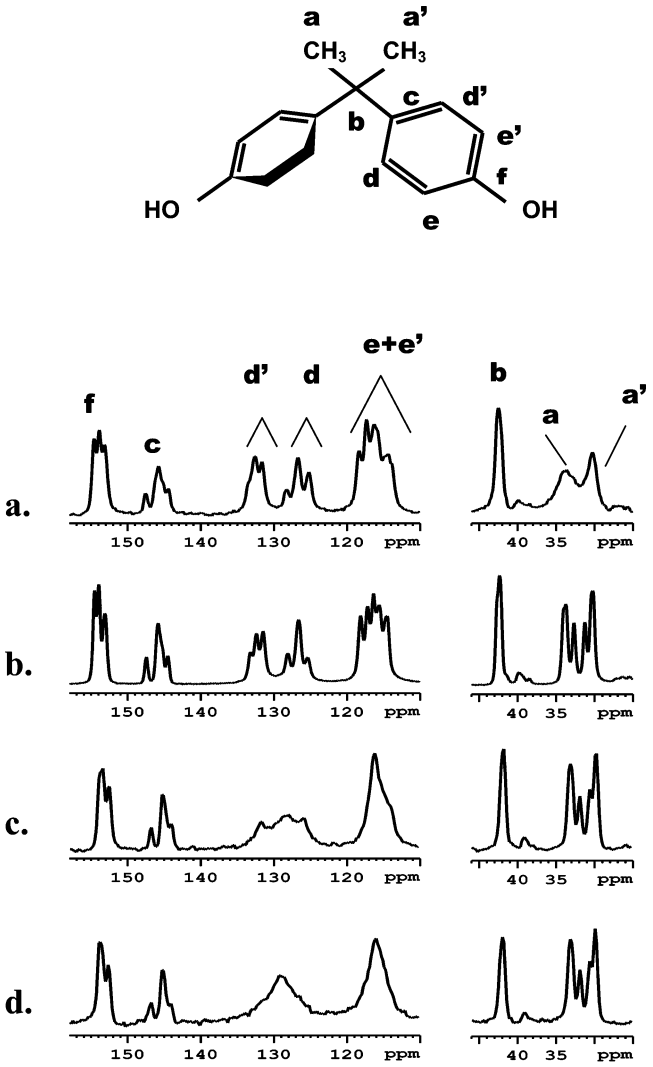

Figure 2. CP/MAS spectra of BPA at (a) −60 °C, (b) 23 °C, (c) 80 °C, and (d) 100 °C. Assignments are indicated on the BPA structure.

Results and Discussion

Figure 1 shows our first experimental result indicating that aromatic ring reorientation occurs in BPA. These results were obtained quite by accident, in that we were deliberately using the crystalline BPA as a control compound for a rigid lattice exchange experiment. As such, we did not expect to observe any cross-peak intensity connecting the diagonal peaks of the protonated aromatic ring carbons. However, Figure 1 clearly shows strong cross peaks connecting the inequivalent ortho ring carbons of BPA, indicating that some form of magnetization transfer or chemical exchange was occurring. Since cross-peaks were observed only between inequivalent ortho or meta aromatic ring signals, and not all ring carbons, this first result suggested a large-amplitude ring flip that interconverted inequivalent ring carbons.

Variable-Temperature CP/MAS Data. Figure 2 shows the CP/MAS ^{13}C spectra of crystalline BPA as a function of temperature, along with a schematic of the molecular structure indicating the chemical shift assignments. Because of its high crystallinity, BPA line widths are narrow and several inequivalent resonances are resolved even at this moderate field strength.

No improvements in resolution were obtained by increasing the ^{13}C Larmor frequency to 125 MHz (data not shown). Examination of the aromatic region (110−160 ppm) of the 23 °C spectrum in Figure 2b indicates that at least three unique signals are observed for each ring carbon, consistent with the X-ray assignment of three inequivalent conformations per unit cell. Closer inspection reveals that the ortho ring carbons d and d′ (125−135 ppm) have six resolved peaks and the meta ring carbons e and e′ (110−120 ppm) give rise to five well-resolved peaks. In fact, the quaternary aromatic carbon c, which has three well-resolved signals, shows evidence for additional inequivalent sites in the asymmetric line shape for the intense 145 ppm signal.

Comparison of the 23 °C result in Figure 2b with spectra obtained at −60 °C (Figure 2a) and 80 °C (Figure 2c) reveal large changes in the peak intensity and resolution for the protonated aromatic ring carbons in the 110−140 ppm region. Specifically, the number of resolved spectral features in this region decreases with increasing temperature. Inspection of the meta carbon region (110−120 ppm) in Figure 2a shows at least seven peaks, relative to five in Figure 2b, and the fourth component of ring carbon c is now apparent relative to the room-temperature result. Additional broadening of the d/d′ carbon region at −60 °C, consistent with the introduction of additional peaks with small chemical shift separations, is also observed. Taken together, these results indicate that a small degree of motional averaging of inequivalent ring carbon positions takes place as the acquisition temperature is increased from −60 to 23 °C. Consideration of the differential packing effects and relative ring plane conformations in each molecule can be used to predict the maximum number of spectral lines observed for each type of ring carbon, in the limit of no motion and infinite spectral resolution. In the low-temperature result of Figure 2a, which was obtained using 100-kHz ^{1}H decoupling, the fact that more than six peaks are observed for the meta carbons e/e′ and more than three peaks are observed for the quarternary ring carbon c indicates that either there is inequivalence between the aromatic ring carbons of each ring in a single molecule or that more than three unique molecular conformations exist in the crystalline unit cell. In the limit of three conformers, and complete inequivalence between the ring carbons of each ring in one molecule, 12 peaks would be expected for the ortho carbons, 12 peaks for the meta carbons, and 6 peaks for each of the quaternary aromatic carbons c and f.

Comparison of Figure 2b with spectra obtained at 80 °C (Figure 2c) and 100 °C (Figure 2d) shows large changes in the spectral patterns for the ortho and meta ring carbons *only*. Coalescence and, ultimately, collapse of each group of inequivalent signals is observed at these elevated temperatures for these off-axis ring carbons. Perturbations in the intensity and resolution of ring carbons c and f are observed, as well as for the inequivalent methyl carbons a and a′, but the effects are small compared to the "fast-exchange" response for protonated ring carbons. The differential averaging of signals indicates a mode of large-amplitude aromatic ring reorientation about the C_2 axis. On the basis of the chemical shift separation of the ortho signal manifold in the static limit of Figure 2a (8 ppm), the minimum exchange rate at the coalescence point observed in 2d is 600 s^{-1}.

2D $^{13}C-^{13}C$ Exchange Data. The data in Figures 1 and 2 indicate that ring dynamics do occur in the crystalline BPA molecule as a function of temperature. However, it is not clear from these data what is the (a) amplitude of the motion vs temperature; (b) relevance of the motion to conformational inequivalence; and (c) sequence of motions, i.e., parallel or concerted vs sequential. Additional 2D NMR experiments as a function of mixing time and temperature have been completed to address these questions. Figure 3 presents the results of 2D ^{13}C exchange experiments at 23 °C and −60 °C. Parts a and b of Figure 3 present the 23 °C results for mixing times of 100 ms and 2s, respectively, while the 100-ms result at −60 °C is shown in Figure 3c. Figure 3a shows that even at relatively short millisecond time scales, ring reorientation that acts to exchange the inequivalent ortho and meta ring carbons among themselves takes place at room temperature. The cross-peak pattern is almost fully developed in Figure 3a, as may be observed by comparison with the 2-s exchange time result in

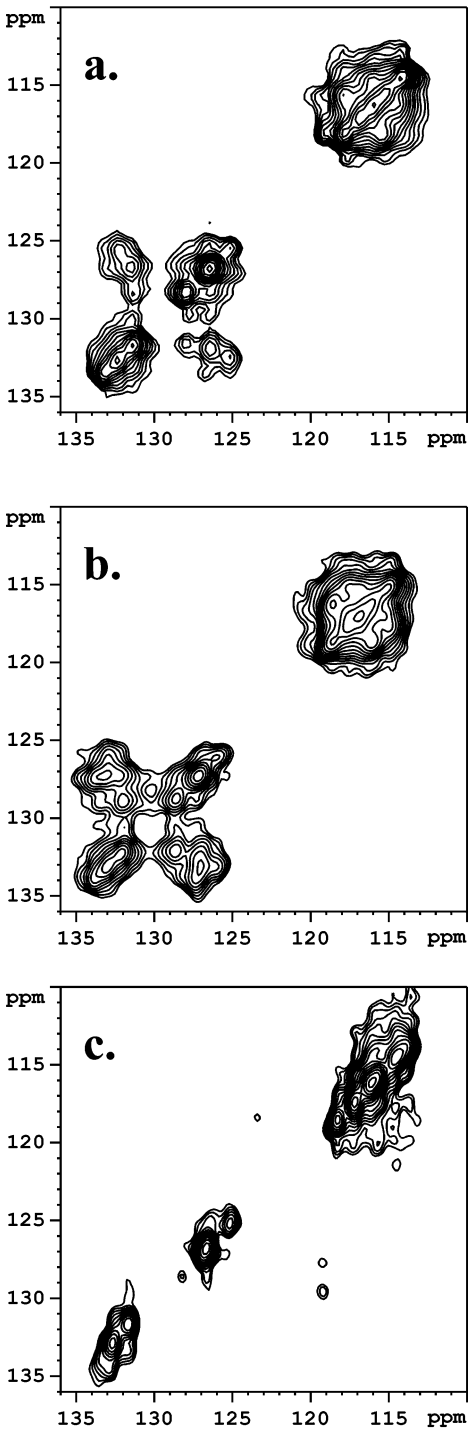

Figure 3. 2D exchange spectra of the aromatic BPA region at (a) 23 °C, 0.1 s exchange; (b) 23 °C, 2 s exchange; and (c) −60 °C, 1 s exchange.

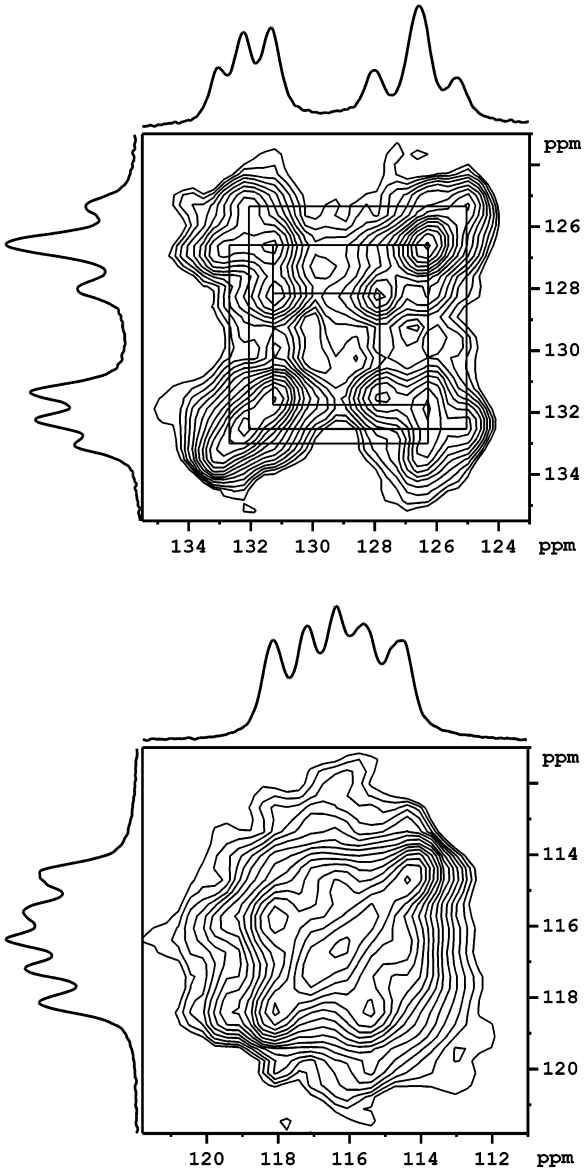

Figure 4. Expanded view of the (a) ortho and (b) meta ring carbons of BPA at 23 °C using a 0.5 s exchange time. In (a), straight lines are used to indicate the exchange pathways. From these, one observes that only two conformers share multiple correlations.

Figure 3b. While the individual cross peaks between the inequivalent ortho ring carbons are well resolved from the diagonal, ring reorientation manifests itself in the meta carbons as broadening of the diagonal. In some cases, individual cross peaks between the e/e′ carbons are apparent. This exchange is quenched on the 100-ms time scale at −60 °C (Figure 3c), and additional experiments with a 2-s exchange time at −60 °C produced a similar spectrum with no cross-peaks (not shown).

An expanded view of the aromatic ring ortho carbon region is shown in Figure 4 for an exchange time of 500 ms at 23 °C. Equilibrium exchange is essentially complete at this mixing time due to equal diagonal and cross-peak intensities. New features are not observed at longer exchange times. Indeed, the individual cross peaks look very similar to the 100-ms result in Figure 3a, albeit with much greater intensity relative to the diagonal. Specifically, four distinct cross peaks may be observed connecting the d/d′ ortho carbons. The fact that more than three cross peaks appear indicates that there are additional conformer dynamics other than just simple exchange of an ortho carbon on one ring (d) to its inequivalent neighbor (d′). The diagonal peaks at 126.2 and 131.3 ppm both show two correlations, while the remaining four peaks only exhibit single cross peaks. The fact that less than nine cross-peaks appear proves that complete interchange between all inequivalent ortho ring positions in all conformers does not occur. Figure 4 proves that in addition to simple exchange of ortho carbons d and d′ within a single conformation, the large-amplitude aromatic ring reorientation facilitates exchange between two of the three different conformers, as shown by the isotropic peaks at 126.2 and 131.3 ppm that exhibit multiple correlations. For example, if one examines the 131.3 ppm peak, two possible events exist. First, the ring motion can exchange an ortho with its ortho′ position, given by the correlation with the 128 ppm peak, or conformer exchange can take place, as indicated by the correlation with the 126.2 ppm peak. A similar situation exists for the 126.2 ppm peak, in that simple ring exchange gives rise to a correlation with the 133 ppm peak. In both cases, the exchange pathway connecting the two inequivalent conformers is one way, i.e., the 128-ppm peak does not correlate with the 133 ppm peak. The conformer represented by the d/d′ isotropic peaks at 125 and 132.3 ppm, respectively, undergoes only ring reorientation.

Exchange Kinetics. The room-temperature kinetic analysis of BPA dynamics is shown in Figure 5, in which the total cross-peak volumes have been plotted vs the mixing time. Since the integrated cross-peak region necessarily contains intensity arising from both ring flips and conformer exchange events, averaged kinetic rate information is obtained. However, since ring flips are the mechanism by which two of the three conformers exchange with one another, this is a physically relevant average. The fact that the 2D exchange data implies two types of exchange events (simple ring flips and ring flip/conformer interchange) is consistent with the fits to the data shown in Figure 5. The dashed single-exponential line does not fit the initial rate but does fit the long-time region. A biexponential fit (solid line) accurately models the initial exchange rate (see inset), as well as longer time events, but does not reproduce the intermediate range data well. Exchange rate constants for the biexponential fit to the equation $y = a(1 - \exp(-k_1x)) + b(1 - \exp(k_2x))$ yielded $k_1 = 0.06\ s^{-1}$ and $k_2 = 0.006\ s^{-1}$. Obviously, higher-order exponentials, or stretched exponentials, could fit all regions of the data. However, the biexponential model is consistent with the physical events revealed in the 1D and 2D exchange NMR data.

Single-Crystal and Powder X-ray Data. The crystalline unit cell of BPA is shown in Figure 6, with color identification of the three inequivalent conformers. The unit cell contains twelve molecules, four each of the three unique conformers. In particular, it appears that the blue and green conformers are more closely equivalent relative to the yellow molecule, as may be observed by inspection of the packing arrangement of each with its neighbors. By inspection of the packing arrangement, it is possible to envision a pairwise molecular flip by which the blue and green conformers relate via a pseudo 4-fold axis. (This would be expected to occur at higher temperatures than those considered in this study.) Other than the expected increase in unit cell volume, the crystal coordinates for single crystals at −60 and 23 °C are equivalent. This confirms that on the time scale of the X-ray experiment (several seconds), the lattice is static. Variable-temperature powder diffraction data, as well as DSC, did not reveal any first-order phase transitions (ambient to 100 °C). However, as expected, thermally induced unit cell expansion was observed from the X-ray powder data as described in Table 1.

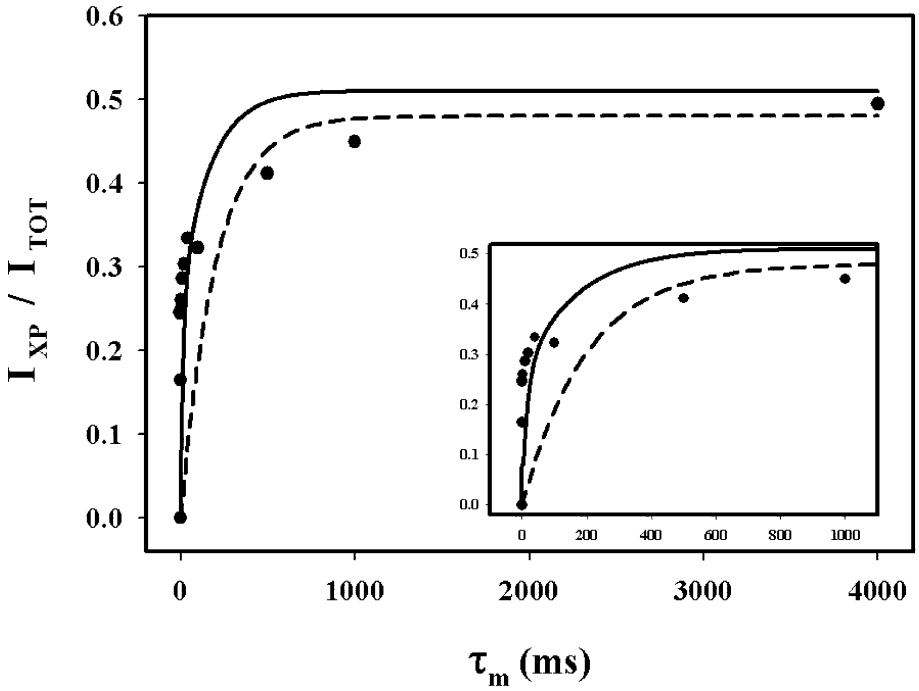

Figure 5. Kinetic plot of the exchange cross peak volume fraction as a function of exchange time (for single (dashed line) and double (line) exponential fits. The equations used in the single and double exponential fits are $y = a(1 - \exp(-k_1x))$ and $y = a(1 - \exp(-k_1x)) + b(1 - \exp(k_2x))$, respectively.

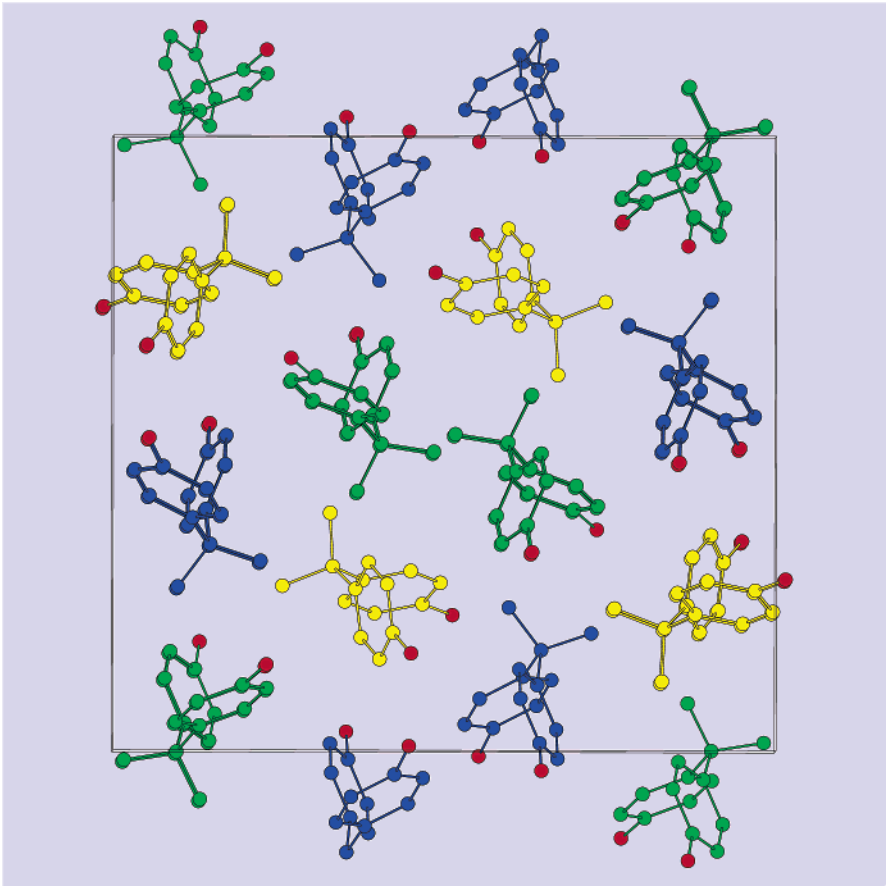

Figure 6. Unit cell structure of BPA, viewed along the *a* axis, derived from the 23 °C single-crystal X-ray data. The three inequivalent molecular conformations are denoted by color.

Simulation of Ring Motions. While the 2D solid-state NMR data unequivocally proves that some type of large-amplitude ring reorientation exists in BPA and that the result of that motion is to interchange inequivalent ortho and meta positions on adjacent rings of the same molecule, it does not reveal the amplitude or relative direction of ring reorientation. If BPA molecules with specific ^{13}C labels at one ortho or meta position were available, then static 2D CSA exchange experiments could

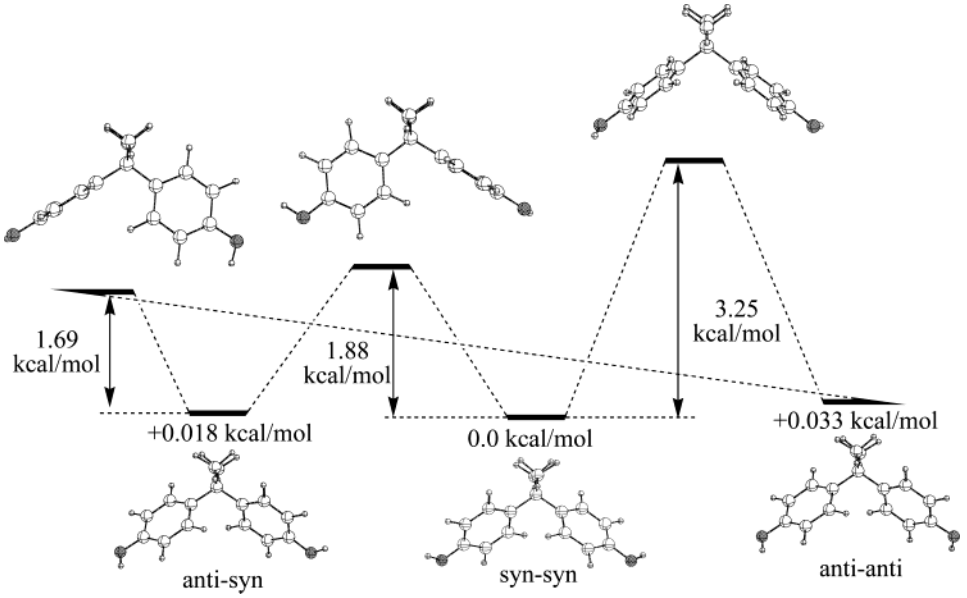

Figure 7. Potential energy diagram for the gas-phase simulation of ring dynamics in isolated BPA molecules, evaluated at the B3LYP/6-31G* level of theory. Energies of the three low-energy equilibrium isomers are shown relative to the lowest-energy isomer. Energies of approximate transition state structures, determined with QST2 methods at the same level of theory, are shown as barrier heights.

TABLE 1

	unit cell volume (nm^3)	
temp (K)	single crystal	powder
213	3.738	
293	3.774[a]	3.728
303		3.769
313		3.778
323		3.790
333		3.793
343		3.820
353		3.824

[a] Obtained from ref 3.

identify the motional amplitude directly.[20] However, in the absence of these expensive models, we have used DFT calculations to evaluate various types of ring motion and construct the corresponding potential energy surfaces for these motions in BPA.

The X-ray data (Figure 6) shows that within a given molecule of BPA, each of the $C-C_{Me}$ bond vectors lie in the same plane as a single aromatic ring. Whether the para-hydroxyl groups on the rings orient themselves syn or anti to the corresponding methyl vectors gives rise to three possible conformational isomers, as confirmed by the gas-phase DFT calculations. Although the syn−syn isomer is calculated to be the lowest in energy, all three are within a few hundredths of a kcal/mol of each other, as shown in Figure 7.

Various types of ring motion will satisfy the requirements of the exchange data in Figures 1−4. DFT calculations revealed that the simple 180° rotation of a given phenyl ring can be broken down into smaller amplitude rotations that effect the same result. As shown in Scheme 1, either a 110° clockwise rotation or a 70° counterclockwise rotation of the highlighted ring will effect the desired exchange. While both rings in BPA are free to utilize either movement, results from Figure 7 show that the lowest-energy movements correspond to both rings moving in the same direction when viewing the molecule along the molecular long axis. This means that one of the phenyl rings will move by 110° while the other moves by 70°, with barrier heights in the range of 1.69−1.88 kcal/mol. Movement of the rings in opposite directions, both through a 70° arc, yields a higher energy barrier of 3.25 kcal/mol.

Some limitations of the theory must be mentioned. First, these results are from gas-phase/isolated molecule calculations. Unfortunately, calculations involving the entire unit cell structure and the associated intermolecular energies are not feasible given the available computational resources. Further, the three conformers identified in the simulations should not necessarily be associated with prediction of the unit cell conformer population, since it is unclear to what extent the hydrogen-bonding network is perturbed when a ring reorients. In other words, the simulations in Figure 7 allowed the phenolic O−H bond vector to move, while this may or may not occur in the crystalline solid state. (Preliminary infrared spectroscopy results indicate that the hydrogen bonding network is also dynamic at room temperature and below.)[23] The three conformers that are identified in the X-ray results differ in slight perturbations of the orientation of the aromatic ring planes relative to the CH_3 bond vector direction, within a molecule. While packing effects may induce these perturbations, which are not described by the simulations, the intramolecular barriers to ring reorientation should rank the possible motions accurately in terms of the ring rotation amplitude.

Scheme 1 illustrates one type of ring motion that contributes to the overall BPA dynamics shown in Figure 7.

SCHEME 1

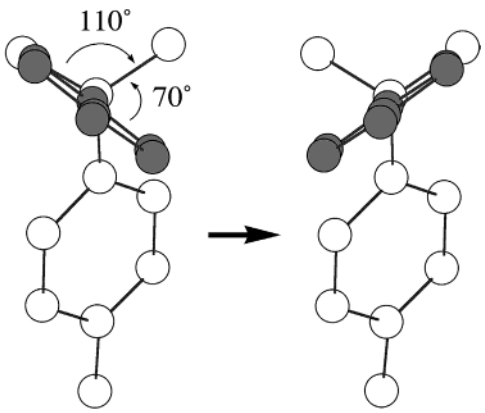

Conclusions

Detailed solid-state NMR experiments have unequivocally revealed the presence of large-amplitude, low-frequency ring reorientations in the crystalline BPA polycarbonate monomer in a manner consistent with recently published reports in other crystalline organic solids.[24,25] In addition to the exchange of magnetically inequivalent ring carbons, this motion allows two of the three inequivalent molecular conformers in the crystalline unit cell to interchange with one another. DFT calculations revealed that the lowest energy pathway for ring dynamics, which satisfied the experimental data, involved concerted rotation of each ring in a molecule by 71 and 110°, respectively, in the same rotation direction. While other rotation modes were found, e.g., opposite rotation of each ring by +71° and −71°, or 180° ring flips, the activation barrier was significantly larger than the 1.8 kcal/mol observed for the preferred motion. Kinetic analysis of the ring dynamics, using the 2D exchange results, was consistent with two disparate exchange phenomena, i.e., equivalent ring flips within a single conformer and ring flips which lead to conformer interchange. Our results indicate that discrete subsets of the overall ring motion previously reported for polycarbonates do take place in the crystalline monomer and act to provide a pathway for conformer exchange between two of the three inequivalent molecular conformations.

Acknowledgment. The authors gratefully acknowledge the National Science Foundation for support of this work under the DMR Grant 0137968 (J.L.W.) and the Instrumentation Grant 9509532 (J.D.M.).

Supporting Information Available: Coordinates from the −60 °C single-crystal X-ray experiments are included as Supporting Information in CIF ascii file format. This material is available free of charge via the Internet at http://pubs.acs.org.

References and Notes

(1) *Chem. Eng. News* **2003**, *81*, 40.
(2) Bel'skii, V. K.; Chernikova, N. Y.; Rotaru, V. K.; Kruchinin, M. M. *Sov. Phys. Crystallogr.* **1983**, *28*, 405.
(3) Okada, K. *J. Mol. Struct.* **1996**, *380*, 223.
(4) X-ray data (lists of atomic coordinates, thermal parameters, structure factors, etc.) acquired at −60 °C is provided as Supporting Information (CIF file).
(5) Schaefer, J.; Stejskal, E. O.; McKay, R. A.; Dixon, W. T. *Macromolecules* **1984**, *17*, 1479.
(6) Lee, P. L.; Schaefer, J. *Macromolecules* **1992**, *25*, 5559.
(7) Schmidt, A.; Schaefer, J. *Macromolecules* **1993**, *26*, 1729.
(8) Kaji, H.; Tai, T.; Horii, F. *Macromolecules* **2001**, *34*, 6318.
(9) Roy, A. K.; Jones, A. A.; Inglefield, P. T. *Macromolecules* **1986**, *19*, 1356.
(10) Spiess, H. W. *Advances in Polymer Science*; Kausch, H. H., Zachmann, H. G., Eds.; Springer-Verlag: Berlin, 1984.
(11) Shi, J. F.; Jones, A. A.; Inglefield, P. T.; Meadows, M. D. *Macromolecules* **1996**, *29*, 605.
(12) Henrichs, P. M.; Russ, H. R. *Macromolecules* **1988**, *21*, 860.
(13) Henrichs, P. M.; Russ, H. R.; Scaringe, R. P. *Macromolecules* **1989**, *22*, 2731.
(14) Schmidt-Rohr, K.; Spiess, H. W. *Multidimensional Solid-State NMR and Polymers*; Academic Press: New York, 1994.
(15) Szeverenyi, N.; Sullivan, M. J.; Maciel, G. E. *J. Magn. Reson.* **1982**, *47*, 462.
(16) Hagemeyer, A.; Schmidt-Rohr, K.; Spiess, H. W. *Adv. Magn. Reson.* **1989**, *13*, 85.
(17) Suter, D.; Ernst, R. R. *Phys. Rev. B* **1985**, *32*, 5608.
(18) van Rossum, B. J.; de Groot, C. P.; Ladishansky, V.; Vega, S.; de Groot, H. J. M. *J. Am. Chem. Soc.* **2000**, *122*, 3465.
(19) Frisch, M. J.; Trucks, G. W.; Schlegel, H. B.; Scuseria, G. E.; Robb, M. A.; Cheeseman, J. R.; Zakrzewski, V. G.; Montgomery, J. A., Jr.; Stratmann, R. E.; Burant, J. C.; Dapprich, S.; Millam, J. M.; Daniels, A. D.; Kudin, K. N.; Strain, M. C.; Farkas, O.; Tomasi, J.; Barone, V.; Cossi, M.; Cammi, R.; Mennucci, B.; Pomelli, C.; Adamo, C.; Clifford, S.; Ochterski, J.; Petersson, G. A.; Ayala, P. Y.; Cui, Q.; Morokuma, K.; Malick, D. K.; Rabuck, A. D.; Raghavachari, K.; Foresman, J. B.; Cioslowski, J.; Ortiz, J. V.; Stefanov, B. B.; Liu, G.; Liashenko, A.; Piskorz, P.; Komaromi, I.; Gomperts, R.; Martin, R. L.; Fox, D. J.; Keith, T.; Al-Laham, M. A.; Peng, C. Y.; Nanayakkara, A.; Gonzalez, C.; Challacombe, M.; Gill, P. M. W.; Johnson, B. G.; Chen, W.; Wong, M. W.; Andres, J. L.; Head-Gordon, M.; Replogle, E. S.; Pople, J. A. *Gaussian 98*, revision A.11; Gaussian, Inc.: Pittsburgh, PA, 1998.
(20) Hariharan, P. C.; Pople, J. A. *Theor. Chim. Acta* **1973**, *28*, 213−222.
(21) Peng, C.; Schlegel, H. B. *Isr. J. Chem.* **1993**, *33*, 449−454.
(22) Kentgens, A. P.; de Boer, E.; Veeman, W. S. *J. Chem. Phys.* **1987**, *87*, 6859.
(23) Folmer, J.; Franzen, S. Private communication.
(24) Harper, J. K.; Facelli, J. C.; Barich, D. H.; McGeorge, G.; Mulgrew, A. E.; Grant, D. M. *J. Am. Chem. Soc.* **2002**, *124*, 10589.
(25) Helluy, X.; Sebald, A. *J. Phys. Chem. B* **2003**, 3290.